HHS Public Access

Author manuscript

Free Radic Biol Med. Author manuscript; available in PMC 2022 October 01.

Published in final edited form as:

Free Radic Biol Med. 2021 October ; 174: 249–263. doi:10.1016/j.freeradbiomed.2021.08.005.

Activation of PPARα-catalase pathway reverses alcoholic liver injury via upregulating NAD synthesis and accelerating alcohol clearance

Ruichao Yue[1], **Guan-yuan Chen**[1], **Guoxiang Xie**[4], **Liuyi Hao**[1], **Wei Guo**[1], **Xinguo Sun**[1], **Wei Jia**[5], **Qibin Zhang**[1,3], **Zhanxiang Zhou**[1,2], **Wei Zhong**[1,2,*]

[1]Center for Translational Biomedical Research, University of North Carolina at Greensboro, North Carolina Research Campus, Kannapolis, NC, USA 28081

[2]Department of Nutrition, University of North Carolina at Greensboro, North Carolina Research Campus, Kannapolis, NC, USA 28081

[3]Department of Chemistry & Biochemistry, University of North Carolina at Greensboro, North Carolina Research Campus, Kannapolis, NC, USA 28081

[4]Shanghai Key Laboratory of Diabetes, Mellitus and Center for Translational Medicine, Shanghai Jiao Tong University Affiliated Sixth People's Hospital, Shanghai 200233, China

[5]Hong Kong Traditional Chinese Medicine Phenome Research Centre, School of Chinese Medicine, Hong Kong Baptist University, Kowloon Tong, Hong Kong 999077, China

Abstract

Alcohol metabolism in the liver simultaneously generates toxic metabolites and disrupts redox balance, but the regulatory mechanisms have not been fully elucidated. The study aimed to characterize the role of PPARα in alcohol detoxification. Hepatic PPARα and catalase levels were examined in patients with severer alcoholic hepatitis. Mouse studies were conducted to determine the effect of PPARα reactivation by Wy14,643 on alcoholic hepatotoxicity and how catalase is involed in mediating such effects. Cell culture study was conducted to determine the effect of hydrogen peroxide on cellular NAD levels. We found that the protein levels of PPARα and catalase were significantly reduced in the livers of patients with severe alcoholic hepatitis. PPARα reactivation by Wy14,643 effectively reversed alcohol-induced liver damage in mice. Global and targeted metabolites analysis revealed a fundamental role of PPARα in regulating the tryptophan-NAD pathway. Notably, PPARα activation completely switched alcohol metabolism from the CYP2E1 pathway to the catalase pathway along with accelerated alcohol clearance. Catalase knockout mice were incompetent in alcohol and hydrogen peroxide clearance

[*]**Corresponding authors**: Wei Zhong, phone: 704-250-5805, w_zhong@uncg.edu.

Author contributions: Z.Z. and W.Z. conception and design of research; R.Y., L.H., W.G., X.S., and W.Z. performed animal experiments and analysis; R.Y. and W.Z. analyzed data and prepared figures; G.C. and Q.Z. analyzed tryptophan metabolites and prepared figures; G.X. and W.J. performed metabolome profiling and prepared figures and tables; R.Y. drafted manuscript.

Conflict of interest: The authors disclose no conflicts.

and were more susceptible to chronic alcohol exposure-induced liver injury. Hydrogen peroxide-treated hepatocytes had a reduced size of cellular NAD pool. These data demonstrate a key role of PPARα in regulating hepatic alcohol detoxification. Catalase-mediated hydrogen peroxide removal represents an underlying mechanism of how PPARα preserves the NAD pool. The study provides a new angle of view about the PPARα-catalase pathway in combating alcohol toxicity.

Graphical Abstract

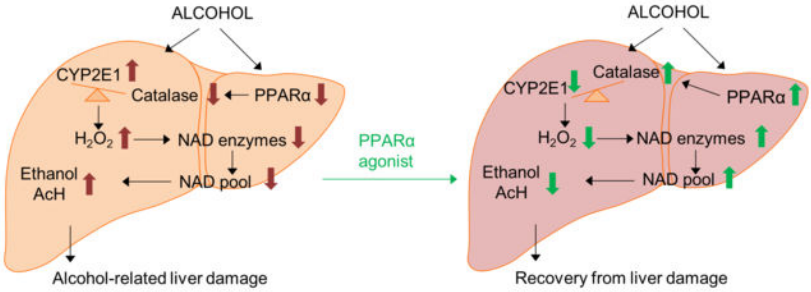

Keywords

Alcohol-related liver disease; PPARα; Catalase; NAD biosynthesis

1. Introduction

Alcohol use disorder remains one of the predominant causes of liver disease and liver-related death worldwide [1, 2]. Heavy drinking can cause increased fat accumulation, inflammation, and over time, irreversible destruction and fibrotic scarring of the liver tissue, which are collectively termed as alcohol-related liver disease (ALD) [1, 3]. However, there are no approved medications for any stage of ALD. Considerable researches have been focused on oxidative stress in alcohol toxicity [4], and antioxidants have been reported to mediate some protective effects in experimental models of ALD [5, 6]. Ethanol and its metabolites have toxic effects on the liver, which contributes to the pathogenesis of ALD. Therefore, understanding the balance of alcohol metabolism and its removal is essential for the exploration of strategies targeting to reduce the accumulation of potentially damaging metabolic byproducts.

The liver is the major organ responsible for metabolizing up to 90% of ingested alcohol [7]. The hepatocytes have three main oxidative pathways, including alcohol dehydrogenase (ADH), cytochrome P450 2E1 (CYP2E1), and catalase, that convert ethanol to acetaldehyde. Aldehyde dehydrogenase 2 (ALDH2) is the major enzyme for metabolizing acetaldehyde to acetate, which is eventually oxidized to carbon dioxide and water [8]. ADH and ALDH reactions involve the conversion of the cofactor nicotinamide adenine dinucleotide (NAD^+) to its reduced form (NADH). As a result, a reduced NAD^+/NADH ratio and a highly reduced cytosolic environment are generated in hepatocytes, which render the cell more susceptible to damage caused by alcohol. Among the 3 ethanol metabolizing enzymes, CYP2E1 is known to be strongly induced by chronic alcohol consumption, leading to elevated oxidative stress [9]. During the catalytic cycle of CYP2E1, a significant amount of

reactive oxygen species (ROS), including hydroxyl radical ($^{\bullet}OH$), superoxide anion ($O_2^{\bullet-}$), and hydrogen peroxide (H_2O_2), is generated. There species can cause toxic effects, such as lipid peroxidation, enzyme inactivation, DNA mutations, and destruction of cell membranes. The catalase pathway, on the contrary, breaks down H_2O_2 into water and oxygen when metabolizing ethanol and has the potential of reducing ROS [10]. Although it has long been considered a minor ethanol metabolizing pathway in the liver, it seems to be important in the brain where ADH is not expressed [11]. Genetic polymorphism in *Catalase* gene influences the susceptibility and severity of alcohol dependence [12]. It has been reported that in the fasting state, catalase-mediated ethanol metabolism is the predominant pathway [13].

Even though it is still unclear how these ethanol metabolizing enzymes are tuned, enhancing the catalase pathway seems to be a promising strategy for a relatively benign alcohol clearance as ROS will be removed as well. Interestingly, many studies reporting a protection against ALD showed a parallel phenomenon of inhibition of hepatic CYP2E1 and induction of catalase [14, 15]. Both CYP2E1 knockout mice and mice treated with CYP2E1 inhibitor are resistant to alcohol-induced fatty liver with a mechanism involves the upregulation of peroxisome proliferator-activated receptor α (PPARα) [16, 17]. PPARα, as a master regulator of peroxisome biogenesis and homeostasis, directly regulates the expression of peroxisomal catalase [18, 19]. PPARα agonists, such as Wy14,643, fenofibrate, and bezafibrate, have been reported to counteract steatosis and fibrosis in a spectrum of murine models of liver diseases, including ALD [20–22]. The major protective mechanism provided by PPARα is about its powerful regulation of fatty acid metabolism [23]. Notably, a previous study has reported that PPARα regulates the key enzymes in NAD^+ biosynthetic pathways [24]. Catalase and NAD^+ are critical components in alcohol metabolism and they are both likely to be regulated by PPARα. These observations drove us to speculate that PPARα may direct participate in alcohol metabolism though regulating catalase and cellular NAD^+ levels.

Here we investigated the effect of PPARα on alcohol metabolism and the reversal effect of PPARα reactivation on alcohol-induced liver damage by its selective agonist, Wy14,643. We performed global and targeted metabolome analysis and characterized the tryptophan-NAD^+ pathway. Using catalase knockout mice, this study was designed to elucidate the role of catalase in PPARα-mediated alcohol clearance. The present study highlights the significance of the PPARα-catalase pathway in NAD biosynthesis and alcohol metabolism, which has long been underestimated.

2. Materials & Methods

2.1. Animal experiments

All animals and procedures were approved by the North Carolina Research Campus Institutional Animal Care and Use Committee (project No. 18003). C57BL/6J mice were purchased from the Jackson Laboratory (Bar Harbor, ME) and catalase knockout mice (CKO; Stock No. 036739-MU; B6.129-Cat^{tm1Ysh}/Mmmh) were obtained from the MMRRC Repository (Davis, CA). For chronic alcohol feeding experiment, twelve-wk old male mice were pair-fed the Lieber-DeCarli liquid diets (Dyets; Bethlehem, PA) containing alcohol (alcohol-fed; AF) or isocaloric maltose dextrin (pair-fed; PF) for 8 wks as previously

described [25]. A PPARα agonist, pirinixic acid (Wy14,643; Cayman Chemical, Ann Arbor, MI), was added to the diets at 25 mg/L for the last wk of the 8-wk feeding. For acute acetaldehyde and/or H_2O_2 intoxication experiment, male C57BL/6J mice were intraperitoneally injected with 100 mg/kg acetaldehyde, 100 mmol/l H_2O_2, or both twice/d for 3 consecutive days.

2.2. Liver samples from patients with alcoholic hepatitis

De-identified liver explant specimens from patients with severe alcoholic hepatitis (SAH) and wedge biopsies from healthy donor livers were collected at Johns Hopkins University under the support of NIAAA-funded Clinical Resource for Alcoholic Hepatitis Investigations (R24AA025017). Descriptive clinical and biochemical data for this cohort have been reported previously [26].

2.3. Cell culture and treatments

Hepa1c1c7 mouse hepatoma cells (American Type Culture Collection/ATCC, Rockville, MD) were grown in Dulbecco's modified eagle medium (Invitrogen, Carlsbad, CA) supplemented with 10% (v/v) fetal bovine serum (Atlanta Biologicals, Lawrenceville, GA), 100 U/ml penicillin and 100 μg/ml streptomycin (Thermo Fisher Scientific, Waltham, MA), at 37°C in a 5% CO2 environment. Confluent cells were treated with 200 μmol/l H_2O_2 (Sigma-Aldrich, St. Louis, MO) for up to 3 h.

2.4. Analysis of liver damage

Serum aminotransferase levels, including alanine aminotransferase (ALT) and aspartate aminotransferase (AST), as indicators of liver injury were measured per the manufacturer's instructions (Thermo Fisher Scientific, Waltham, MA). Liver sections with hematoxylin and eosin (H&E) staining were examined by light microscopy to determine histopathological changes.

2.5. Lipid analysis in the blood and liver

Serum levels of triglyceride and free fatty acids (FFAs) were determined by quantification kits from BioVision (Milpitas, CA). Hepatic lipids were extracted using chloroform/methanol (2:1), evaporated, and dissolved in 5% triton X-100. Triglyceride and FFAs contents were determined using colorimetric assay kits from BioVision (Milpitas, CA).

2.6. Immunohistochemistry

Paraffin-embedded liver sections were handled using standard methods as described previously [27]. The following antibodies were used for immunoblotting: anti-PPARα (Thermo Fisher Scientific), anti-4-HNE (Northwest Life Science Specialties, Vancouver, WA), anti-CHOP (Cell Signaling Technology, Danvers, MA), anti-catalase (EMD Millipore, Burlington, MA), anti-CYP2E1 (Abcam, Cambridge, MA), anti-NADSYN (Antibodies-online, Limerick, PA), anti-TDO2 (Thermo Fisher Scientific), and anti-NMNAT1 (Lifespan Biosciences, Seattle, WA). Methyl green was used to counterstain cell nuclei for 4-HNE staining.

2.7. Immunofluorescence

Cryostat liver sections from control subjects and SAH patients were incubated with anti-PPARα or anti-catalase antibody followed by Alexa Fluor 594-conjugated donkey anti-rat IgG (Jackson ImmunoResearch Laboratories, West Grove, PA). The nuclei were counterstained by 4',6-diamidino-2-phenylindole (DAPI; Thermo Fisher Scientific).

2.8. Hepatic metabolomic profiles

Liver samples were prepared and analyzed with high-performance liquid chromatography time-of-flight mass spectrometry (HPLC-TOFMS) [28]. Compound identification was performed by comparing the accurate mass and retention time with reference standard or the Human Metabolome Database (http://www.hmdb.ca/).

2.9. PPARα and catalase activities

Liver nuclear extracts were prepared using a nuclear extraction kit from Cayman Chemical. PPARα activity in the extracts was assessed by detecting double-stranded DNA-bound PPARα with specific antibodies in an ELISA format (Cayman Chemical). Catalase activity in whole liver homogenates was examined using a catalase activity assay kit (BioVision). The following antibodies were used for immunoblotting: anti-PPARα (Thermo Fisher Scientific), anti-4-HNE (Northwest Life Science Specialties, Vancouver, WA), anti-CHOP (Cell Signaling Technology, Danvers, MA), anti-catalase (EMD Millipore, Burlington, MA), anti-CYP2E1 (Abcam, Cambridge, MA), anti-NADSYN (Antibodies-online, Limerick, PA), anti-TDO2 (Thermo Fisher Scientific), and anti-NMNAT1 (Lifespan Biosciences, Seattle, WA). Methyl green was used to counterstain cell nuclei for 4-HNE staining.

2.10. Measurement of ethanol and acetaldehyde

Ethanol and acetaldehyde levels in mouse serum and livers were measured using headspace gas chromatography–mass spectrometry (GC-MS; Agilent Technologies, Santa Clara, CA). All samples were stored at −80°C prior analysis and were processed at 4°C to minimize evaporation. Briefly, 100 μl serum was analyzed with 100 mg sodium chloride and 10 μmol n-propanol as the internal control. One hundred mg liver was homogenized in 300 μl water containing 10 μmol n-propanol. Supernatant after centrifugation was transferred to testing vail for analysis. GC-MS analysis was carried out using an Agilent 7890A GC and 5975C MS with CTC-PAL autosampler equipped with headspace sampling module (Agilent Technologies). The mass spectrometer was operated in single ion monitoring mode with the following ions monitored: acetaldehyde 1.60–3.0 min m/z 29, 43 and 44, ethanol 3.0–5.0 min m/z 31, 45 and 46, and n-propanol 5.0–11.0 min m/z 31, 59 and 60.

2.11. Detection of H_2O_2

Hydrogen peroxide levels in the serum and livers were measured with the Amplex Red hydrogen peroxide assay kit (Thermo Fisher Scientific). Amplex Red reagent reacted with H_2O_2 in the samples to produce the red oxidation product, resorufin, which can be measured at OD = 560 nm.

2.12. Quantification of nicotinamide adenine dinucleotide

Total nicotinamide adenine dinucleotide (NAD), NAD^+, and NADH in liver samples or cells were measured using NAD^+/NADH quantification colorimetric kit per the manufacturer's instructions (BioVision).

2.13. Measurement of tryptophan metabolites

Hepatic tryptophan metabolites were measured by Vanquish UHPLC coupled with Quantiva triple quadrupole mass spectrometer (Thermo Fisher Scientific, Haverhill, MA). The method and identification of each metabolite has been previously reported [29]. A list of detected tryptophan metabolites is summarized in Table S3.

2.14. RNA extraction and RT-qPCR

RNA was isolated from liver by using TRIzol reagent (Thermo Fisher Scientific), and reverse transcribed to cDNAs. Quantitative PCR (qPCR) reactions were performed using cDNA mix with primers in RT^2 Real-Time SYBR Green/ROX master mix (Qiagen, Germantown, MD) on an Applied Biosystems 7500 PCR system (Carlsbad, CA). Primers were designed and synthesized by Integrated DNA Technologies (Coralville, CA), and listed in Table S4.

2.15. Western blot

Mouse livers homogenates were loaded onto 12% sodium dodecyl sulfate-polyacrylamide gel, transblotted onto polyvinylidene difluoride membranes (Bio-Rad, Hercules, CA), blocked with 5% nonfat dry milk, and then incubated with the following antibodies, including anti-PPARα, anti-TDO2 (Thermo Fisher Scientific), anti-catalase (EMD Millipore), anti-CYP2E1, anti-ADH, anti-ALDH2, anti-NQO1 (Abcam), anti-GSTM1 (Proteintech, Rosemont, IL), anti-ATF4, anti-GAPDH (Cell Signaling Technology), anti-NADSYN (Antibodies-online), anti-NMNAT1 (Lifespan Biosciences) and anti-β-actin (Sigma-Aldrich, St. Louis, MO). The membranes were then incubated with HRP-conjugated goat anti-rabbit IgG, goat anti-mouse IgG, or rabbit anti-goat IgG (Thermo Fisher Scientific). The bound complexes were detected by enhanced chemiluminescence and quantified by densitometry analysis.

2.16. Statistical analysis

All data are expressed as mean ± standard deviation (SD). The results were analyzed by Student's *t*-test or one-way analysis of variance (ANOVA) followed by Student-Newman-Keuls test. Differences between groups were considered significant at $P < 0.05$.

3. Results

3.1. Pharmacological activation of PPARα reverses alcohol-induced liver damage

Hepatic PPARα dysfunction has been observed in a number of experimental models of ALD. Here, in the present study, we first examined the livers of patients with SAH by Western blot and immunofluorescence staining and found that the patients had over 60% reduction in PPARα protein levels and less nuclear distribution (Fig. 1A). We then

experimentally reactivated PPARα through administrating a PPARα agonist, Wy14,643, to mice for 1 wk in an 8-wk alcohol feeding protocol to test the reversal effects on alcohol-induced liver damage. Administration of Wy14,643 restored alcohol-reduced protein levels of PPARα (Fig. 1B) as well as its activity and distribution (Fig. S1A). Alcohol-induced elevation of serum ALT and AST was completely normalized by Wy14,643 administration (Fig. 1C). Wy14,643 administration also improved alcohol-induced lipid accumulation and hepatocyte necrotic degeneration as indicated by cell enlargement and nuclear disappearance (Fig. 1D). With restored PPARα activity, mice had lower levels of hepatic cytokine/chemokine, including *Cxcl1*, *Mcp1*, and *Tnfα*, and reduced levels of 4-HNE compared with alcohol-fed (AF) mice (Fig. S1B–C). We examined the enzymes involved in cellular protein against oxidative stress, including NQO1 and GSTM1. Alcohol exposure led to the induction of nicotinamide quinone oxidoreductase (NQO1) and glutathione-S-transferase (GSTM1) by 3- to 4-fold, which was reversed by PPARα activation (Fig. S1D). It is known that PPARα is a master regulator of lipid metabolism and its activation lowers lipid levels [23]. Indeed, administration of PPARα agonist dramatically reduced blood and hepatic triglyceride and free fatty acid levels regardless of alcohol exposure (Table S1). Moreover, PPARα activation also conciliated alcohol-induced ER stress as indicated by normalized ATF4 and CHOP levels (Fig. 1E). In contrast to strong positive staining of CHOP in AF mice, especially around the veins, a significant reduction of CHOP signals were detected in mice with Wy14,643 administration (Fig. 1F). Collectively, the data indicate that pharmacological reactivation of PPARα reverses alcohol-induced liver damage.

3.2. Activation of PPARα rebalances alcohol-perturbed hepatic metabolome especially tryptophan metabolism

The findings presented above suggested that the role of PPARα includes but not limited to regulating lipid metabolism, so we performed hepatic metabolite profiling to better characterize the impacts of PPARα activation, especially in the context of alcohol exposure. A total of 197 metabolites in liver samples were identified by HPLC-TOFMS, of which 166 metabolites were significantly changed by either alcohol or Wy14,643 or both. Compared to AF mice, Wy14,643-administrated AF mice had 101 metabolites significantly altered. Alcohol exposure perturbed 97 metabolites in control groups and only 36 metabolites in Wy14,643 groups. Among the 97 alcohol-perturbed metabolites, 56 metabolites were further altered by Wy14,643, which were summarized in Table 1. Impressively, activation of PPARα normalized 50 out of 56 metabolites. These metabolites range from lipids, organic acids, nucleosides, benzenoids, organic nitrogen compounds, organic oxygen compounds, and organic heterocyclic compounds. There were 3 metabolites that were increased by alcohol and further increased by Wy14,643, including pyruvic acid, 3-phosphoglyceric acid, and urocanic acid (marked in red), and 3 metabolites that were decreased by alcohol and further decreased by Wy14,643, including 5,8,11,14,17-eicosapentaenoic acid, 6-phosphogluconic acid, and urocanic acid (marked in blue). Unsupervised analysis of the metabolomes showed that AF group had the most significant trend of separation from the other 3 groups (Fig. 2A). Subsequent pathway analysis comparing the effect of PPARα agonist between the 2 AF groups found 35 significantly altered pathways (Table S2). Interestingly, the most significantly changed pathways are all related to tryptophan metabolism (Fig. 2B).

The above finding motivated us to perform targeted tryptophan metabolite analysis. We detected 22 tryptophan metabolites in mouse livers (Fig. 2C). Like metabolome profiling, the clusters of tryptophan metabolites of AF group clearly separated from the other 3 groups, whereas Wy14,643 administration driven the clusters more closely to PF controls, suggesting improved tryptophan metabolism (Fig. 2D). Alcohol exposure decreased tryptophan levels and increased kynurenine (KYN), kynurenic acid (KYNA), and anthranilic acid (AA) levels in mouse liver, whereas activation of PPARα effectively reversed these effects (Fig. 2E). Activation of PPARα also changed other tryptophan metabolites, including xanthurenic acid (XA), picolinic acid (PA; Fig. 2E), indole-3-ethanol (IET), serotonin (SER), indole-3-lactic acid (ILA), and indole-3-acetic acid (I3AA; Fig. S2), compared to AF only mice. Two dietary tryptophan metabolites, nicotinamide (NAM) and nicotinic acid (NA), were also both higher in PPARα agonist-treated AF mice than those in AF only mice (Fig. 2E).

3.3. Activation of PPARα dramatically increases NAD levels in the liver

As summarized in Fig. S3A, data from tryptophan metabolites analysis suggested that alcohol exposure disrupts NAD^+ de novo synthesis with accumulation of KYN, KYNA, and AA, whereas administration of PPARα agonist not only improves *de novo* NAD^+ biosynthesis, but may also elevate cellular NAD^+ levels through the Preiss-Handler pathway from NA or through the salvage pathway from NAM. We measured hepatic NAD^+/NADH levels and found that alcohol exposure decreased cellular NAD^+ and total NAD levels as well as the ratio of NAD^+/NADH (Fig. 3A). NAD^+ levels was dramatically elevated by PPARα activation, which was even higher when combined with alcohol. As a result, Wy14,643-treated PF mice had much higher NAD^+/NADH ratio compared to control PF mice, but the 2 AF groups showed similar NAD^+/NADH ratio due to increased NADH levels in Wy14,643-treated AF mice (Fig. 3A). We measured the expression of a panel of enzymes involved in NAD biosynthesis. Among all 13 genes measured, 8 enzymes were downregulated after alcohol exposure, including *Kyn*, *Haao*, *Nmnat1*, *Nmnat2*, *Nadsyn1*, *Nadk*, *Naprt*, and *Nnt*, most of which were reversed to normal or even higher than normal levels by Wy14,643 (Fig. 3B). Tryptophan 2,3-dioxygenase (TDO2) was the only alcohol-upregulated enzyme detected. It catalyzes the first and rate-limiting step of the kynurenine pathway. PPARα activation further upregulated TDO2. Western blot analysis confirmed that administration of Wy14,643 led to profound induction of TDO2 in the livers of mice (Fig. 3C). Glutamine-dependent NAD^+ synthetase (NADSYN) was also induced by Wy14,643. Histological examination showed that TDO2 induced by Wy14,643 was mainly distributed within the hepatocyte cytoplasm, whereas Wy14,643-induced NADSYN was more dominant in the hepatocyte nuclei (Fig. 3D). Although the protein levels of NMNAT1 remained unchanged (Fig. 3C), its distribution was unevenly perturbed by alcohol and was significantly increased in the hepatocyte nuclei after Wy14,643 administration (Fig. S3B).

3.4. Activation of PPARα upregulates hepatic catalase and speeds up ethanol and H_2O_2 clearance

It is well-known that alcohol metabolism lowers cellular NAD^+/NADH redox ratio [4, 9]. Therefore, we next determined the effect of PPARα activation on ethanol clearance. Notably, administration of Wy14,643 significantly reduced serum ethanol levels by 69%

and hepatic ethanol levels by over 95% (Fig. 4A). Hepatic acetaldehyde levels were also dropped after Wy14,643 administration (Fig. 4A). To our surprise, administration of Wy14,643 totally blocked alcohol-induced CYP2E1 in the livers of mice as well as inhibiting the protein levels of ADH and ALDH2 (Fig. 4B). On the contrary, catalase was significantly induced by PPARα activation (Fig. 4B). This PPARα-mediated metabolic switch from CYP2E1 to catalase was further confirmed by immunohistochemistry staining (Fig. 4C). Activity analysis showed that alcohol exposure resulted in over 35% reduction of hepatic catalase activity, whereas administration of Wy14,643 elevated its activity by 43–65% compared to PF only control (Fig. 4D). Because CYP2E1 pathway generates ROS and catalase pathway consumes ROS, H_2O_2 levels in the serum and liver were measured. Surprisingly, alcohol-induced H_2O_2 accumulation in the serum and liver were both effectively cleared to normal levels by PPARα activation (Fig. 4E). These results indicate a key role of PPARα in speeding up ethanol and H_2O_2 clearance possibly through activating catalase.

3.5. Knockout of catalase hinders hepatic ethanol clearance through increasing H_2O_2 levels and reducing NAD pool

To confirm a concomitant change of catalase with PPARα inactivation in the livers of patients with SAH, hepatic catalase protein levels were measured. As shown in Figure 5A, Western blot analysis and immunofluorescence staining showed that the levels of hepatic catalase were significantly reduced in SAH patients compared with controls. To explore the role of catalase in PPARα-mediated alcohol clearance, a mouse strain deficient in catalase was subjected to chronic alcohol feeding. Hepatic protein levels of alcohol metabolizing enzymes were measured by Western blot. Alcohol feeding reduced hepatic catalase, a similar trend as observed in human ALD, whereas no catalase was detectable in knockout mice regardless of alcohol feeding (Fig. 5B). Catalase knockout mice had comparable hepatic CYP2E1 induction and similar ADH levels but higher ALDH2 levels than WT mice upon alcohol intoxication (Fig. 5B). Alcohol-induced H_2O_2 accumulation was further elevated by catalase deletion (Fig. 5C). Moreover, catalase deficiency caused a significant reduction in hepatic NAD^+ and NADH levels, which had synergistic effect with alcohol intoxication (Fig. 5D). The NAD^+/NADH ratio, however, was only reduced by alcohol rather than by catalase knockout (Fig. 5D). We then analyzed ethanol and acetaldehyde levels and found that catalase knockout mice not only had more ethanol accumulation in the blood and livers than WT mice, but also had higher levels of acetaldehyde in both organs examined (Fig. 5E).

3.6. Hydrogen peroxide directly reduces cellular NAD levels and hinders alcohol clearance

To define the role of H_2O_2 in cellular NAD levels and alcohol clearance, we examined NAD biosynthesis in catalase knockout mouse model of ALD and in cell culture studies and tested alcohol clearance in an acute model of acetaldehyde and H_2O_2 exposure. We first measured NAD biosynthesis enzymes and found that catalase knockout mice expressed higher levels of hepatic TDO2 and NADSYN compared with WT mice (Fig. 6A). However, both enzymes as well as NMNAT1 were significantly reduced by alcohol. The mRNA levels of *Tdo2*, *Kmo*, *Haao*, *Nmnat1*, *Nmnat2*, *Nadsyn1*, *Nampt*, *Nmrk1*, *Naprt*, *Idh2*, and *Nnt*

were all upregulated in catalase knockout mice compared with WT mice, alcohol exposure further elevated the expression of *Nmrk1* and *Naprt* and downregulated *Tdo2* and *Nmnat1* (Fig. 6B). We then exposed Hepa1c1c7 cells with 200 μmol/l H_2O_2 for up to 3h. Hydrogen peroxide treatment significantly reduced cellular NAD^+ levels for all indicated time points and slightly reduced NADH levels at 30 min (Fig. 6C). The NAD^+/NADH ratio was also decreased in cells treated with H_2O_2 over the experimental period (Fig. 6C). Next, we performed an acute experiment by giving WT mice acetaldehyde with or without H_2O_2. Although H_2O_2 alone did not alter blood ethanol or acetaldehyde levels, co-treatment with acetaldehyde significantly augmented the levels of both (Fig. 6D), suggesting that H_2O_2 is a potent inhibitor hampering alcohol metabolism.

3.7. Mice deficient in catalase are more susceptible to alcohol-induced liver damage

In association with inhibited H_2O_2 and alcohol clearance, mice deficient in catalase had higher serum ALT levels than WT mice after alcohol exposure (Fig. 7A). Alcohol-induced hepatocyte necrotic degeneration, as indicated by enlarged cell size and nucleus disappearance, and lipid accumulation were more frequently detected in the liver sections of catalase knockout mice than in WT mice (Fig. 7B). Hepatic mRNA levels of *Mcp1* and *Tnfα* were upregulated by alcohol and further increased by catalase knockout (Fig. 7C). Alcohol-induced *Cxcl1*, however, was blunted in catalase knockout mice (Fig. 7C). Lipid peroxidation in the liver was increased by alcohol and aggregated by catalase knockout as indicated by 4-HNE staining (Fig. 7D). Catalase knockout mice had a spontaneous induction in antioxidative enzymes, such as NQO1 and GSTM1 which were both further increased by alcohol (Fig. 7E). To determine the effect of peroxisomal catalase deficiency on organelle homeostasis, we examined ER stress markers ATF4 and CHOP. After alcohol exposure, WT mice expressed substantially higher protein levels of ATF4 and CHOP, which were significantly augmented by catalase knockout (Fig. 7F). The increase in CHOP protein levels was further confirmed by immunohistochemistry staining, and catalase knockout mice had more CHOP accumulation, especially around the veins, after alcohol exposure (Fig. 7F). Taken together, mice deficient in catalase are more vulnerable to alcohol-induced hepatic inflammation, oxidative stress, and organelle damage, such as ER stress.

4. Discussion

This study demonstrated that short term activation of PPARα with concomitant alcohol exposure effectively reversed alcoholic hepatotoxicity in an chronic alcohol intoxication mouse model. The PPARα agonist was as added to the diets at 25 mg/L, which is lower than the dosages used in many previous studies [30–32]. Although activation of PPARα has been reported to protect the liver from diseases, such as nonalcoholic steatohepatitis [33], alcoholic liver disease [20, 32], and nutritional fibrosis [31], these studies focus on the role of PPARα in regulating lipid homeostasis and/or inflammatory responses. In the present study, we found a profound effect of PPARα on speeding up alcohol clearance with a complete switch of ethanol metabolism from the ROS-generating CYP2E1 pathway to the ROS-scavenging catalase pathway (summarized in Fig. 8). We further found that PPARα regulates the expression of NAD biosynthesis enzymes, therefore promoting tryptophan metabolism and NAD biosynthesis. As a PPARα target, catalase consumes

H_2O_2, which helps in reducing ROS and maintaining cellular NAD levels. These may serve as a central and fundamental mechanism for speeding up the clearance of alcohol and ROS and alleviating liver damage elicited by PPARα activation. Coincidentally, a recent study reported that Wy14,643 treatment dramatically lowered serum ethanol levels through induction of catalase [34]. In that study, injection of catalase inhibitor increased serum ethanol levels, whereas knockout of PPARα blunted the effects of Wy14,643. Here, in our study, we report that the effect of Wy14,643 on alcohol metabolism is not only restricted to the ethanol-to-acetaldehyde step but also to the conversion of acetaldehyde into acetate. A discrepancy is that Wy14,643 exacerbated alcohol-induced liver injury despite of accelerated alcohol metabolism in that study [34]. The duration of Wy14,643 treatment, the degree of PPARα activation, and the sensitivity of mouse strains could all be factors affecting the outcomes.

Our study provides new insight into a comprehensive role of PPARα in regulating cellular metabolism, particularly the tryptophan - NAD metabolism. PPARα is highly expressed in the liver and acts as a master regulator of lipid metabolism [23]. Through global metabolome profiling, we found that PPARα activation compellingly corrected almost all alcohol-perturbed metabolites. Subsequent targeted tryptophan metabolites quantification and NAD enzyme analysis indicate that PPARα directly regulates the gene expression of multiple enzymes related to NAD biosynthesis. Moreover, PPARα activation upregulated hepatic catalase and accelerated H_2O_2 disposal, which helped in preserving the NAD pool size. A previous study reported that PPAR agonists increased hepatic NAD^+ levels in Sprague-Dawley rats in concert with increased activity of quinolinate phosphoribosyl transferase (QPRT) and inhibited expression of aminocarboxymuconate-semialdehyde decarboxylase (ACMSD) [24]. However, we did not detect significant changes in the mRNA levels of either enzymes regardless of alcohol or PPARα agonist treatment (data not shown). Instead, we found that PPARα activation dramatically upregulated TDO2 and NADSYN regardless of alcohol exposure. TDO2 is the rate-limiting enzyme directing the conversion of tryptophan to kynurenine [30]. Its induction in alcohol-fed mice explains the accumulation of kynurenine detected in this study. NADSYN catalyzes the final step in NAD biosynthesis [35]. One of the unexpected findings is that PPARα increased the distributions of NADSYN and NMNAT1 in hepatocyte nucleus. This suggests that PPARα is important for compartmentalized NAD^+ biosynthesis and function considering the subcellular localization of many NAD^+-consuming enzymes, such as sirtuins and poly (ADP-ribose) polymerases [35–37]. It is known that ethanol oxidation increases is response its concentration and is raised to near saturation levels of ADH due to the limited bioavailability of NAD^+ [38]. Since an increase in NADH is detrimental to ADH and ALDH activities, maintaining the normal redox state (NAD^+/NADH ratio) through re-oxidation of NADH or elevation in NAD^+ biosynthesis is pivotal to the cells under the condition of ethanol. Given the fact that the cellular NAD^+/NADH ratio is decreased due to alcohol metabolism, the regulation of NAD biosynthesis by PPARα has profound effects on multiple metabolic pathways that require NAD^+ or are inhibited by NADH in the pathogenesis of ALD.

In addition to stimulating NAD biosynthesis, PPARα activation accelerated alcohol clearance in chronic model of ALD in mice. The induction of catalase, increased NAD biosynthesis, and rebalanced NAD^+/NADH ratio all benefit and promote this process.

Reactions mediated by ADH and ALDH2 both reduce NAD^+ to NADH [9], so an improved cellular NAD^+/NADH ratio is pivotal to the disposal of ethanol and its toxic metabolite, acetaldehyde [39, 40], and pushes the reactions to produce acetate. This may explain why Wy14,643 administration also reduced acetaldehyde levels in mouse livers. It is noteworthy that Wy14,643 did not change acetaldehyde levels in the blood at the indicated time. Based on the dramatically reduced hepatic and serum ethanol levels as well as decreased hepatic acetaldehyde levels, it is predictable that Wy14,643 would also promotes systemic acetaldehyde clearance over time. Multiple measurements at different time points may better characterizing the kinetics. In addition, we found that catalase deficiency resulted in impaired acetaldehyde clearance and ALDH2 adaptive induction upon alcohol intoxication. Therefore, it seems that PPARα orchestrates both the reactions of ethanol to acetaldehyde and acetaldehyde to acetate. Our group previously reported that pharmacological activation of ALDH2 reverses alcohol-induced hepatic steatosis and cell injury in mice [25]. On the other hand, ALDH2 knockout mice have significantly higher levels of blood ethanol and acetaldehyde [41], impaired glucose metabolism [40], and accelerated alcohol-induced liver inflammation and fibrosis [42]. In the present study, although ALDH2 protein levels were slightly induced in catalase knockout mice, it was still not enough to compensate the accumulation of acetaldehyde and ethanol due to catalase and NAD deficiency. These experimental studies point to a possibly of harnessing alcohol metabolism for the treatment of ALD. We found that hepatic PPARα-catalase pathway is significantly compromised in patients with SAH and in mouse models of ALD, which may represent a central mechanism of alcohol-induced liver damages, such as ER stress and inflammation, through accumulation of ethanol and acetaldehyde.

One of the most interesting findings in the study is that PPARα activation led to a thoroughly metabolic switch from the CYP2E1 pathway to the catalase pathway. Despite intensive focus on alcohol pharmacokinetics and metabolism, numerous questions remain to be elucidated, including the factors regulating alcohol metabolism *in vivo*, outcomes of metabolic switch between the ethanol metabolizing enzymes though they all convert ethanol to acetaldehyde, and the molecular mechanisms involved in such metabolic switch. The study presents direct evidence that increased levels of H_2O_2 induced by catalase knockout promote NAD deficiency, hamper alcohol metabolism, and accelerate liver damage induced by alcohol, suggesting a protective role of catalase in combating ROS during the progression of ALD. CYP2E1, on the contrary, favors ROS production, such as $^{\bullet}OH$, $O_2^{\bullet-}$, and most importantly, H_2O_2 [4]. Previous studies using CYP2E1 knockout mice or CYP2E1 inhibitor, chlormethiazole, found a significant induction of hepatic PPARα and a consequential protection against alcohol-induced fatty liver [16, 17]. It seems that a negative feedback loop exists between the PPARα-catalase pathway and the CYP2E1-ROS signaling. Moreover, improved redox balance would also preserve hepatic aldehyde detoxifying enzymes, which in turn, facilitates aldehyde clearance, including acetaldehyde and lipid aldehydes. Indeed, we detected ALDH2 reduction after PPARα activation and induction of it in catalase knockout mice exposed to alcohol. Future studies are needed to reveal what is the mechanism/molecule orchestrating the balance and to ascertain how such balance can be maintained upon alcohol intoxication.

Although catalase is 1 of the 3 enzymes responsible for ethanol metabolism, few studies have investigated the involvement of catalase in ALD pathogenesis. In the present study, we found that mice with catalase deficiency are more vulnerable to alcohol-induced damage, including aggregated ER stress, inflammation, and oxidative stress. This is consistent with earlier findings in the fields of ALD and nonalcoholic liver disease. Harrison-Findik *et. al* reported a synergistic induction of ER stress by alcohol and H_2O_2 in the absence of catalase or glutathione peroxidase 1 [43]. In models of nonalcoholic liver disease, knockdown of catalase depressed mitochondrial biogenesis and accelerated lipid accumulation [44, 45]. The effects of catalase knockout on organelle damage would be predicted to relate to the accumulation of H_2O_2 and subsequent amplification of H_2O_2-dependent signal transduction pathways or oxidant damage. Catalase is localized to the peroxisome and functions as an antioxidant enzyme by converting H_2O_2 to oxygen and water [46]. ER is physically and metabolically connected with peroxisomes [47, 48]. Catalase deficiency-induced oxidative stress may directly result in ER stress or indirectly impair ER homeostasis via defective peroxisomes that resulted in the accumulation of peroxisomal proteins in the ER [49, 50].

In summary, our study reports a reversal effect of pharmacological activation of PPARα on ALD pathogenesis. It reveals an emerging role of PPARα in switching alcohol metabolism from ROS-generating CYP2E1 pathway to ROS-scavenging catalase pathway in a mouse model of ALD. Mechanistic study demonstrates that the PPARα-catalase pathway plays an important role in regulating NAD biosynthesis enzymes, maintaining NAD^+/NADH redox balance, and thereby speeding up alcohol removal and H_2O_2 detoxification. The findings establish proof-of-concept for the use of PPARα-catalase activators in ALD therapy.

Supplementary Material

Refer to Web version on PubMed Central for supplementary material.

Acknowledgments

Grant support: This work was supported by National Institutes of Health (R21AA026062 to W.Z., R01AA020212 and R01AA018844 to Z.Z.).

Abbreviations:

ACMSD	aminocarboxymuconate-semialdehyde decarboxylase
ADH	alcohol dehydrogenase
AF	alcohol-fed
ALD	alcohol-related liver disease
ALDH2	aldehyde dehydrogenase 2
ALT	alanine aminotransferase
AST	aspartate aminotransferase
CYP2E1	cytochrome P450 2E1

GSTM1	glutathione-S-transferase
HAAO	3-hydroxyanthranilate 3,4-dioxygenase
IDH2	isocitrate dehydrogenase 2
KMO	kynurenine 3-Monooxygenase
KYNU	kynureninase
NAD	nicotinamide adenine dinucleotide
NADK	NAD^+ kinase
NADSYN	glutamine-dependent NAD^+ synthetase
NAMPT	nicotinamide phosphoribosyltransferase
NAPRT	nicotinate phosphoribosyltransferase
NMNAT1	nicotinamide mononucleotide adenylyltransferase 1
NMRK1	nicotinamide riboside kinase 1
NNT	nicotinamide nucleotide transhydrogenase
NQO1	nicotinamide quinone oxidoreductase
PF	pair-fed
PPARα	peroxisome proliferator-activated receptor α
QPRT	quinolinate phosphoribosyl transferase
SAH	severe alcoholic hepatitis
ROS	reactive oxygen species
TDO2	tryptophan 2,3-dioxygenase

References

[1]. Gao B, Bataller R, Alcoholic liver disease: pathogenesis and new therapeutic targets, Gastroenterology141(5) (2011) 1572–85. [PubMed: 21920463]

[2]. Rowe IA, Lessons from Epidemiology: The Burden of Liver Disease, Digestive diseases35(4) (2017) 304–309. [PubMed: 28468017]

[3]. Altamirano J, Bataller R, Alcoholic liver disease: pathogenesis and new targets for therapy, Nature reviews. Gastroenterology & hepatology8(9) (2011) 491–501. [PubMed: 21826088]

[4]. Wu D, Cederbaum AI, Oxidative stress and alcoholic liver disease, Seminars in liver disease29(2) (2009) 141–54. [PubMed: 19387914]

[5]. Arteel GE, Oxidants and antioxidants in alcohol-induced liver disease, Gastroenterology124(3) (2003) 778–90. [PubMed: 12612915]

[6]. Han KH, Hashimoto N, Fukushima M, Relationships among alcoholic liver disease, antioxidants, and antioxidant enzymes, World journal of gastroenterology22(1) (2016) 37–49. [PubMed: 26755859]

[7]. Zakhari S, Overview: how is alcohol metabolized by the body?, Alcohol research & health : the journal of the National Institute on Alcohol Abuse and Alcoholism29(4) (2006) 245–54. [PubMed: 17718403]

[8]. Jiang Y, Zhang T, Kusumanchi P, Han S, Yang Z, Liangpunsakul S, Alcohol Metabolizing Enzymes, Microsomal Ethanol Oxidizing System, Cytochrome P450 2E1, Catalase, and Aldehyde Dehydrogenase in Alcohol-Associated Liver Disease, Biomedicines8(3) (2020).

[9]. Cederbaum AI, Alcohol metabolism, Clinics in liver disease16(4) (2012) 667–85. [PubMed: 23101976]

[10]. Handler JA, Thurman RG, Redox interactions between catalase and alcohol dehydrogenase pathways of ethanol metabolism in the perfused rat liver, The Journal of biological chemistry265(3) (1990) 1510–5. [PubMed: 2295642]

[11]. Zimatkin SM, Deitrich RA, Ethanol metabolism in the brain, Addiction biology2(4) (1997) 387–400. [PubMed: 26735944]

[12]. Plemenitas A, Kastelic M, Porcelli S, Serretti A, Rus Makovec M, Kores Plesnicar B, Dolzan V, Genetic variability in CYP2E1 and catalase gene among currently and formerly alcohol-dependent male subjects, Alcohol and alcoholism50(2) (2015) 140–5. [PubMed: 25514903]

[13]. Handler JA, Thurman RG, Hepatic ethanol metabolism is mediated predominantly by catalase-H2O2 in the fasted state, FEBS letters238(1) (1988) 139–41. [PubMed: 3169246]

[14]. Yan SL, Yang HT, Lee HL, Yin MC, Protective effects of maslinic acid against alcohol-induced acute liver injury in mice, Food and chemical toxicology : an international journal published for the British Industrial Biological Research Association74 (2014) 149–55. [PubMed: 25301236]

[15]. Senthilkumar R, Viswanathan P, Nalini N, Effect of glycine on oxidative stress in rats with alcohol induced liver injury, Die Pharmazie59(1) (2004) 55–60. [PubMed: 14964423]

[16]. Lu Y, Zhuge J, Wang X, Bai J, Cederbaum AI, Cytochrome P450 2E1 contributes to ethanol-induced fatty liver in mice, Hepatology47(5) (2008) 1483–94. [PubMed: 18393316]

[17]. Zeng T, Zhang CL, Song FY, Zhao XL, Xie KQ, CMZ reversed chronic ethanol-induced disturbance of PPAR-alpha possibly by suppressing oxidative stress and PGC-1alpha acetylation, and activating the MAPK and GSK3beta pathway, PloS one9(6) (2014) e98658. [PubMed: 24892905]

[18]. Toyama T, Nakamura H, Harano Y, Yamauchi N, Morita A, Kirishima T, Minami M, Itoh Y, Okanoue T, PPARalpha ligands activate antioxidant enzymes and suppress hepatic fibrosis in rats, Biochemical and biophysical research communications324(2) (2004) 697–704. [PubMed: 15474484]

[19]. Shin MH, Lee SR, Kim MK, Shin CY, Lee DH, Chung JH, Activation of Peroxisome Proliferator-Activated Receptor Alpha Improves Aged and UV-Irradiated Skin by Catalase Induction, PloS one11(9) (2016) e0162628. [PubMed: 27611371]

[20]. Nakajima T, Kamijo Y, Tanaka N, Sugiyama E, Tanaka E, Kiyosawa K, Fukushima Y, Peters JM, Gonzalez FJ, Aoyama T, Peroxisome proliferator-activated receptor alpha protects against alcohol-induced liver damage, Hepatology40(4) (2004) 972–80. [PubMed: 15382117]

[21]. Nan YM, Kong LB, Ren WG, Wang RQ, Du JH, Li WC, Zhao SX, Zhang YG, Wu WJ, Di HL, Li Y, Yu J, Activation of peroxisome proliferator activated receptor alpha ameliorates ethanol mediated liver fibrosis in mice, Lipids in health and disease12 (2013) 11. [PubMed: 23388073]

[22]. Kong L, Ren W, Li W, Zhao S, Mi H, Wang R, Zhang Y, Wu W, Nan Y, Yu J, Activation of peroxisome proliferator activated receptor alpha ameliorates ethanol induced steatohepatitis in mice, Lipids in health and disease10 (2011) 246. [PubMed: 22208561]

[23]. Varga T, Czimmerer Z, Nagy L, PPARs are a unique set of fatty acid regulated transcription factors controlling both lipid metabolism and inflammation, Biochimica et biophysica acta1812(8) (2011) 1007–22. [PubMed: 21382489]

[24]. Shin M, Ohnishi M, Iguchi S, Sano K, Umezawa C, Peroxisome-proliferator regulates key enzymes of the tryptophan-NAD+ pathway, Toxicology and applied pharmacology158(1) (1999) 71–80. [PubMed: 10387934]

[25]. Zhong W, Zhang W, Li Q, Xie G, Sun Q, Sun X, Tan X, Sun X, Jia W, Zhou Z, Pharmacological activation of aldehyde dehydrogenase 2 by Alda-1 reverses alcohol-induced hepatic steatosis and cell death in mice, Journal of hepatology62(6) (2015) 1375–81. [PubMed: 25543082]

[26]. Weeks SR, Sun Z, McCaul ME, Zhu H, Anders RA, Philosophe B, Ottmann SE, Garonzik Wang JM, Gurakar AO, Cameron AM, Liver Transplantation for Severe Alcoholic Hepatitis, Updated Lessons from the World's Largest Series, Journal of the American College of Surgeons226(4) (2018) 549–557. [PubMed: 29409981]

[27]. Sun Q, Zhang W, Zhong W, Sun X, Zhou Z, Dietary Fisetin Supplementation Protects Against Alcohol-Induced Liver Injury in Mice, Alcoholism, clinical and experimental research40(10) (2016) 2076–2084.

[28]. Zhong W, Li Q, Xie G, Sun X, Tan X, Sun X, Jia W, Zhou Z, Dietary fat sources differentially modulate intestinal barrier and hepatic inflammation in alcohol-induced liver injury in rats, American journal of physiology. Gastrointestinal and liver physiology305(12) (2013) G919–32. [PubMed: 24113767]

[29]. Chen GY, Zhong W, Zhou Z, Zhang Q, Simultaneous determination of tryptophan and its 31 catabolites in mouse tissues by polarity switching UHPLC-SRM-MS, Analytica chimica acta1037 (2018) 200–210. [PubMed: 30292294]

[30]. Cheong JE, Sun L, Targeting the IDO1/TDO2-KYN-AhR Pathway for Cancer Immunotherapy - Challenges and Opportunities, Trends in pharmacological sciences39(3) (2018) 307–325. [PubMed: 29254698]

[31]. Ip E, Farrell G, Hall P, Robertson G, Leclercq I, Administration of the potent PPARalpha agonist, Wy-14,643, reverses nutritional fibrosis and steatohepatitis in mice, Hepatology39(5) (2004) 1286–96. [PubMed: 15122757]

[32]. Fischer M, You M, Matsumoto M, Crabb DW, Peroxisome proliferator-activated receptor alpha (PPARalpha) agonist treatment reverses PPARalpha dysfunction and abnormalities in hepatic lipid metabolism in ethanol-fed mice, The Journal of biological chemistry278(30) (2003) 27997–8004. [PubMed: 12791698]

[33]. Larter CZ, Yeh MM, Van Rooyen DM, Brooling J, Ghatora K, Farrell GC, Peroxisome proliferator-activated receptor-alpha agonist, Wy 14,643, improves metabolic indices, steatosis and ballooning in diabetic mice with non-alcoholic steatohepatitis, Journal of gastroenterology and hepatology27(2) (2012) 341–50. [PubMed: 21929649]

[34]. Chen X, Xu Y, Denning KL, Grigore A, Lu Y, PPARalpha agonist WY-14,643 enhances ethanol metabolism in mice: Role of catalase, Free radical biology & medicine169 (2021) 283–293. [PubMed: 33892114]

[35]. Canto C, Menzies KJ, Auwerx J, NAD(+) Metabolism and the Control of Energy Homeostasis: A Balancing Act between Mitochondria and the Nucleus, Cell metabolism22(1) (2015) 31–53. [PubMed: 26118927]

[36]. Canto C, Sauve AA, Bai P, Crosstalk between poly(ADP-ribose) polymerase and sirtuin enzymes, Molecular aspects of medicine34(6) (2013) 1168–201. [PubMed: 23357756]

[37]. Ryu KW, Nandu T, Kim J, Challa S, DeBerardinis RJ, Kraus WL, Metabolic regulation of transcription through compartmentalized NAD(+) biosynthesis, Science360(6389) (2018).

[38]. Matsuzaki S, Gordon E, Lieber CS, Increased alcohol dehydrogenase independent ethanol oxidation at high ethanol concentrations in isolated rat hepatocytes: the effect of chronic ethanol feeding, The Journal of pharmacology and experimental therapeutics217(1) (1981) 133–7. [PubMed: 7009832]

[39]. Setshedi M, Wands JR, Monte SM, Acetaldehyde adducts in alcoholic liver disease, Oxidative medicine and cellular longevity3(3) (2010) 178–85. [PubMed: 20716942]

[40]. Gao Y, Zhou Z, Ren T, Kim SJ, He Y, Seo W, Guillot A, Ding Y, Wu R, Shao S, Wang X, Zhang H, Wang W, Feng D, Xu M, Han E, Zhong W, Zhou Z, Pacher P, Niu J, Gao B, Alcohol inhibits T-cell glucose metabolism and hepatitis in ALDH2-deficient mice and humans: roles of acetaldehyde and glucocorticoids, Gut68(7) (2019) 1311–1322. [PubMed: 30121625]

[41]. Kiyoshi A, Weihuan W, Mostofa J, Mitsuru K, Toyoshi I, Toshihiro K, Kyoko K, Keiichi N, Iwao I, Hiroshi K, Ethanol metabolism in ALDH2 knockout mice--blood acetate levels, Legal medicine11Suppl 1 (2009) S413–5. [PubMed: 19356968]

[42]. Kwon HJ, Won YS, Park O, Chang B, Duryee MJ, Thiele GE, Matsumoto A, Singh S, Abdelmegeed MA, Song BJ, Kawamoto T, Vasiliou V, Thiele GM, Gao B, Aldehyde

dehydrogenase 2 deficiency ameliorates alcoholic fatty liver but worsens liver inflammation and fibrosis in mice, Hepatology60(1) (2014) 146–57. [PubMed: 24492981]

[43]. Harrison-Findik DD, Lu S, The effect of alcohol and hydrogen peroxide on liver hepcidin gene expression in mice lacking antioxidant enzymes, glutathione peroxidase-1 or catalase, Biomolecules5(2) (2015) 793–807. [PubMed: 25955433]

[44]. Shin SK, Cho HW, Song SE, Bae JH, Im SS, Hwang I, Ha H, Song DK, Ablation of catalase promotes non-alcoholic fatty liver via oxidative stress and mitochondrial dysfunction in diet-induced obese mice, Pflugers Archiv : European journal of physiology471(6) (2019) 829–843. [PubMed: 30617744]

[45]. Hwang I, Uddin MJ, Pak ES, Kang H, Jin EJ, Jo S, Kang D, Lee H, Ha H, The impaired redox balance in peroxisomes of catalase knockout mice accelerates nonalcoholic fatty liver disease through endoplasmic reticulum stress, Free radical biology & medicine148 (2020) 22–32. [PubMed: 31877356]

[46]. Ho YS, Xiong Y, Ma W, Spector A, Ho DS, Mice lacking catalase develop normally but show differential sensitivity to oxidant tissue injury, The Journal of biological chemistry279(31) (2004) 32804–12. [PubMed: 15178682]

[47]. Lodhi IJ, Semenkovich CF, Peroxisomes: a nexus for lipid metabolism and cellular signaling, Cell metabolism19(3) (2014) 380–92. [PubMed: 24508507]

[48]. Horner SM, Liu HM, Park HS, Briley J, Gale M Jr., Mitochondrial-associated endoplasmic reticulum membranes (MAM) form innate immune synapses and are targeted by hepatitis C virus, Proceedings of the National Academy of Sciences of the United States of America108(35) (2011) 14590–5. [PubMed: 21844353]

[49]. Kim PK, Mullen RT, Schumann U, Lippincott-Schwartz J, The origin and maintenance of mammalian peroxisomes involves a de novo PEX16-dependent pathway from the ER, The Journal of cell biology173(4) (2006) 521–32. [PubMed: 16717127]

[50]. Kovacs WJ, Charles KN, Walter KM, Shackelford JE, Wikander TM, Richards MJ, Fliesler SJ, Krisans SK, Faust PL, Peroxisome deficiency-induced ER stress and SREBP-2 pathway activation in the liver of newborn PEX2 knock-out mice, Biochimica et biophysica acta1821(6) (2012) 895–907 [PubMed: 22441164]

Highlights

- PPARα promotes ethanol and acetaldehyde clearance.
- PPARα-activation switches ethanol metabolism from ROS-generating CYP2E1 pathway to ROS-scavenging catalase pathway
- The PPARα-catalase pathway regulates NAD biosynthesis and NAD^+/NADH redox balance.

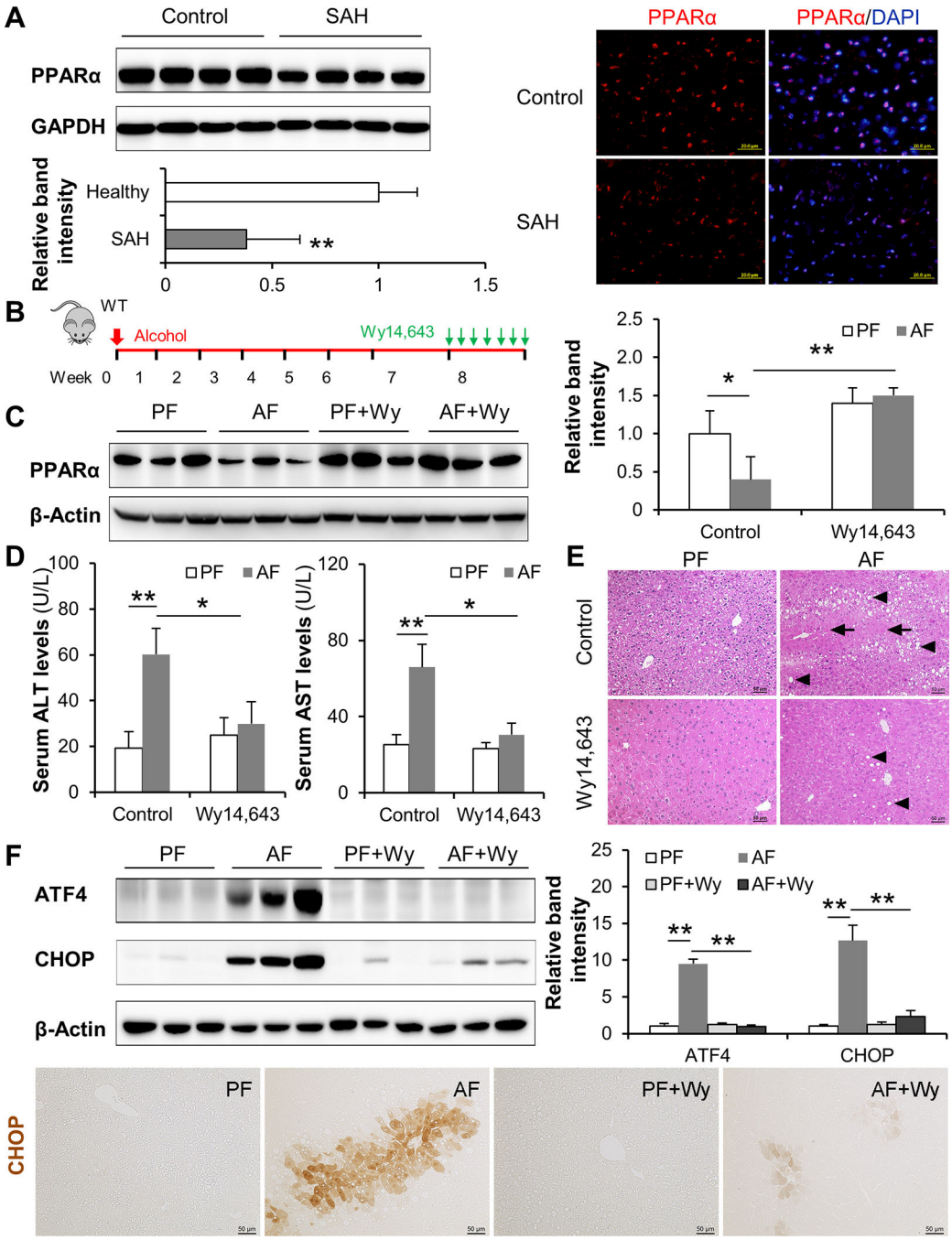

Figure 1. Alcohol induces hepatic PPARα dysfunction in humans and mice and PPARα activation reverses alcohol-induced liver damage in mice.

WT mice were pair-fed control or alcohol diet with or without a PPARα agonist, Wy14,643, supplementation at 25 mg/L for the last wk in an 8-wk feeding experiment. (A) Western blot and immunofluorescence staining of PPARα in the livers of control subjects and patients with SAH (n=4). (B) Experimental design of alcohol feeding and Wy14,643 treatment in mice. (C) Representative Western blot bands and quantification of hepatic PPARα in mice. (D) Serum ALT and AST levels (n=9). (E) Hematoxylin and eosin (H&E) staining of liver sections. Arrowheads indicate lipid accumulation and arrows indicate hepatocyte

degeneration. Scale bar, 50 μm. (F) Representative Western blot bands and quantification of ER stress markers, ATF4 and CHOP, in the liver. IHC staining of CHOP in liver sections. Scale bar, 50 μm. *P<0.05, **P<0.01. PF, pair-fed; AF, alcohol-fed; Wy, Wy14,643; SAH, severe alcoholic hepatitis.

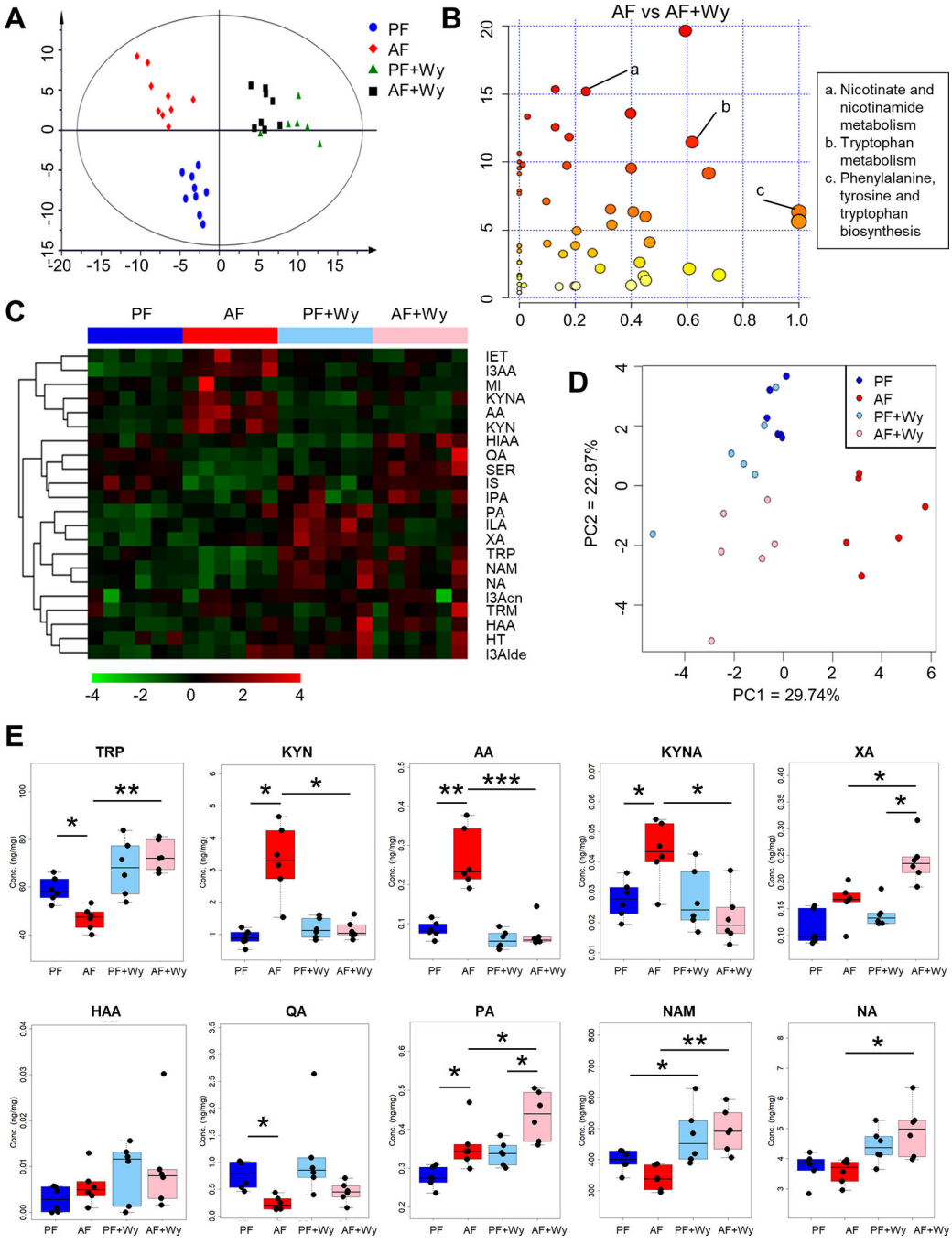

Figure 2. PPARα activation alters hepatic metabolome, especially tryptophan metabolism, that is perturbed by alcohol in mice.

WT mice were pair-fed control or alcohol diet with or without a PPARα agonist, Wy14,643, supplementation at 25 mg/L for the last wk in an 8-wk feeding experiment. (A) Principal component analysis (PCA) of hepatic metabolites in mice measured by HPLC-TOFMS (n=9). (B) Summary of pathway analysis of hepatic metabolomes comparing AF and AF+Wy14,643 groups. (C) Heatmap of 22 tryptophan metabolites in the livers of mice detected by Vanquish UHPLC coupled with Quantiva triple quadrupole mass spectrometer (n=6). (D) PCA of hepatic tryptophan metabolites. (E) Quantification of individual

tryptophan metabolites in the livers of mice. *P<0.05, **P<0.01, ***P<0.001. PF, pair-fed; AF, alcohol-fed; Wy, Wy14,643.

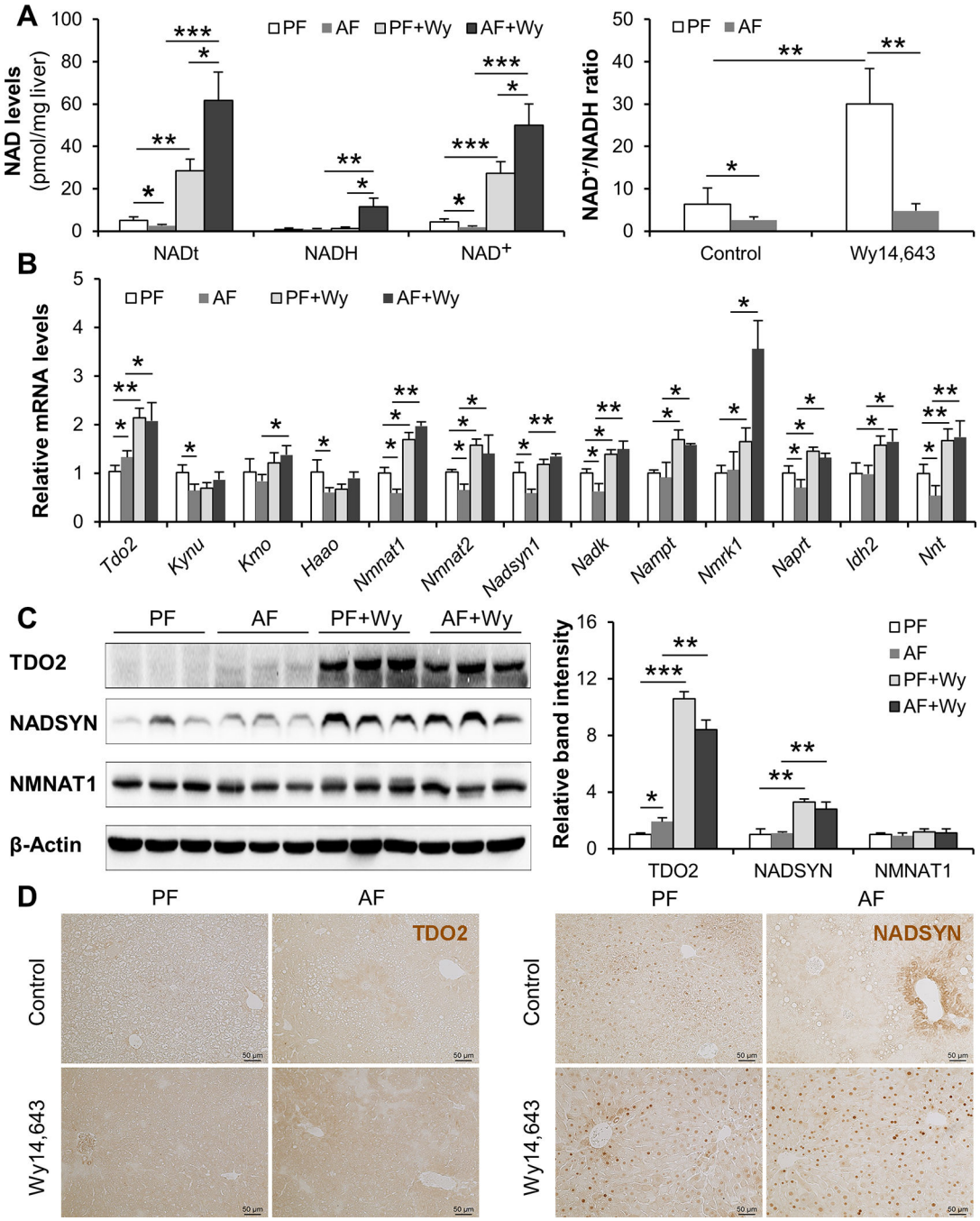

Figure 3. PPARα activation rebalances alcohol-perturbed hepatic NAD levels and NAD biosynthesis enzymes in mice.

WT mice were pair-fed control or alcohol diet with or without a PPARα agonist, Wy14,643, supplementation at 25 mg/L for the last wk in an 8-wk feeding experiment. (A) Hepatic total NAD, NAD^+, NADH levels and NAD^+/NADH ratio (n=6). (B) mRNA levels of enzymes involved in NAD biosynthesis measured by qPCR (n=4). (C) Representative Western blot bands and quantification of NAD biosynthesis enzymes TDO2, NADSYN, and NMNAT1. (D) IHC staining of TDO2 and NADSYN in liver sections. Scale bar, 50 μm. *P<0.05, **P<0.01, ***P<0.001. PF, pair-fed; AF, alcohol-fed; Wy, Wy14,643.

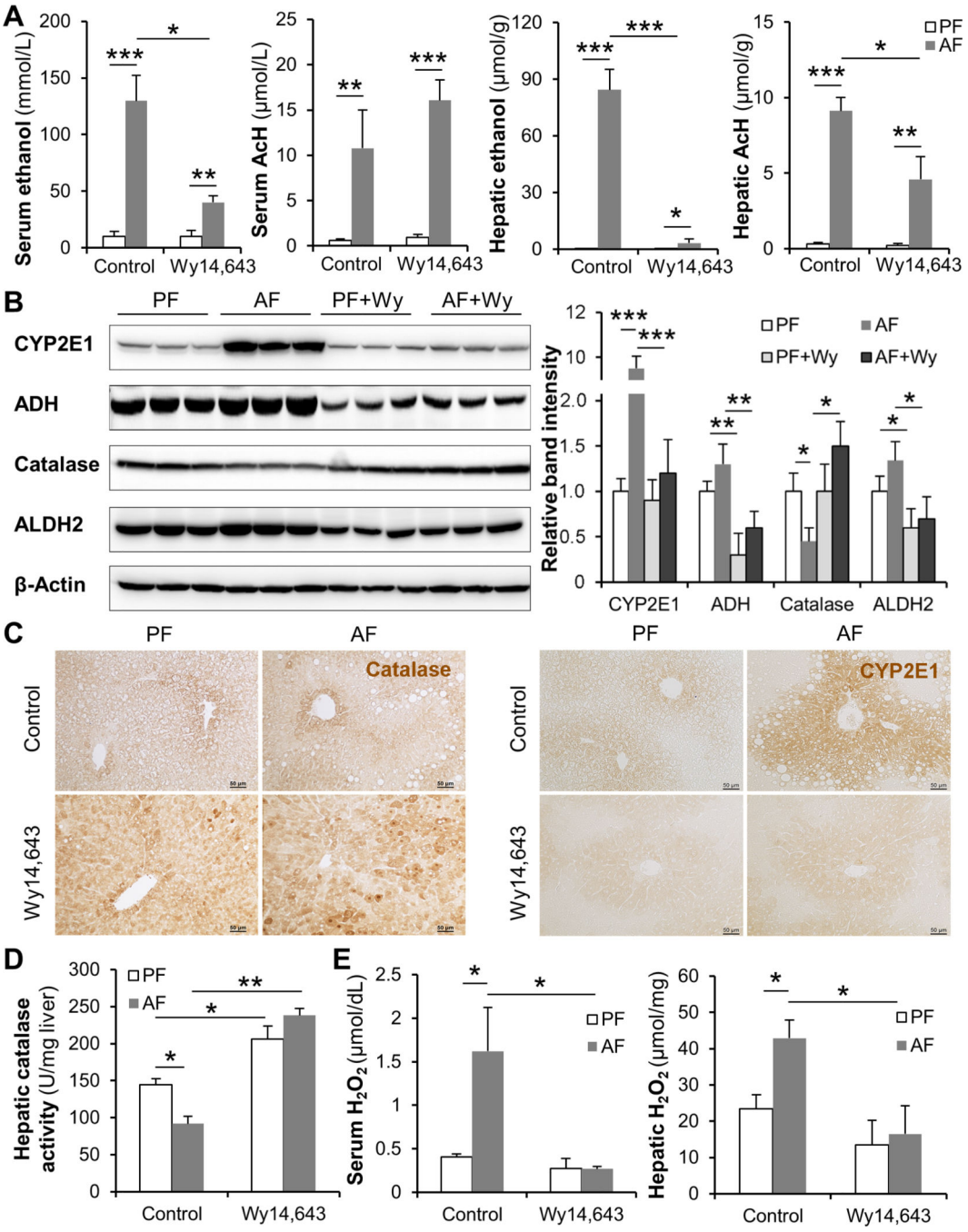

Figure 4. PPARα activation speeds up alcohol and H_2O_2 clearance in mice.

WT mice were pair-fed control or alcohol diet with or without a PPARα agonist, Wy14,643, supplementation at 25 mg/L for the last wk in an 8-wk feeding experiment. (A) Blood and hepatic ethanol and acetaldehyde levels quantified by GC-MS (n=6). (B) Representative Western blot bands and quantification of alcohol metabolizing enzymes CYP2E1, ADH, catalase and ALDH2. (C) IHC staining of catalase and CYP2E1 in liver sections. Scale bar, 50 μm. (D) Hepatic catalase activity calculated as units per mg liver (n=6). (E) Blood and

hepatic H_2O_2 levels measured using Amplex Red H_2O_2 assay kit (n=6). *P<0.05, **P<0.01, ***P<0.001. PF, pair-fed; AF, alcohol-fed; Wy, Wy14,643; AcH, acetaldehyde.

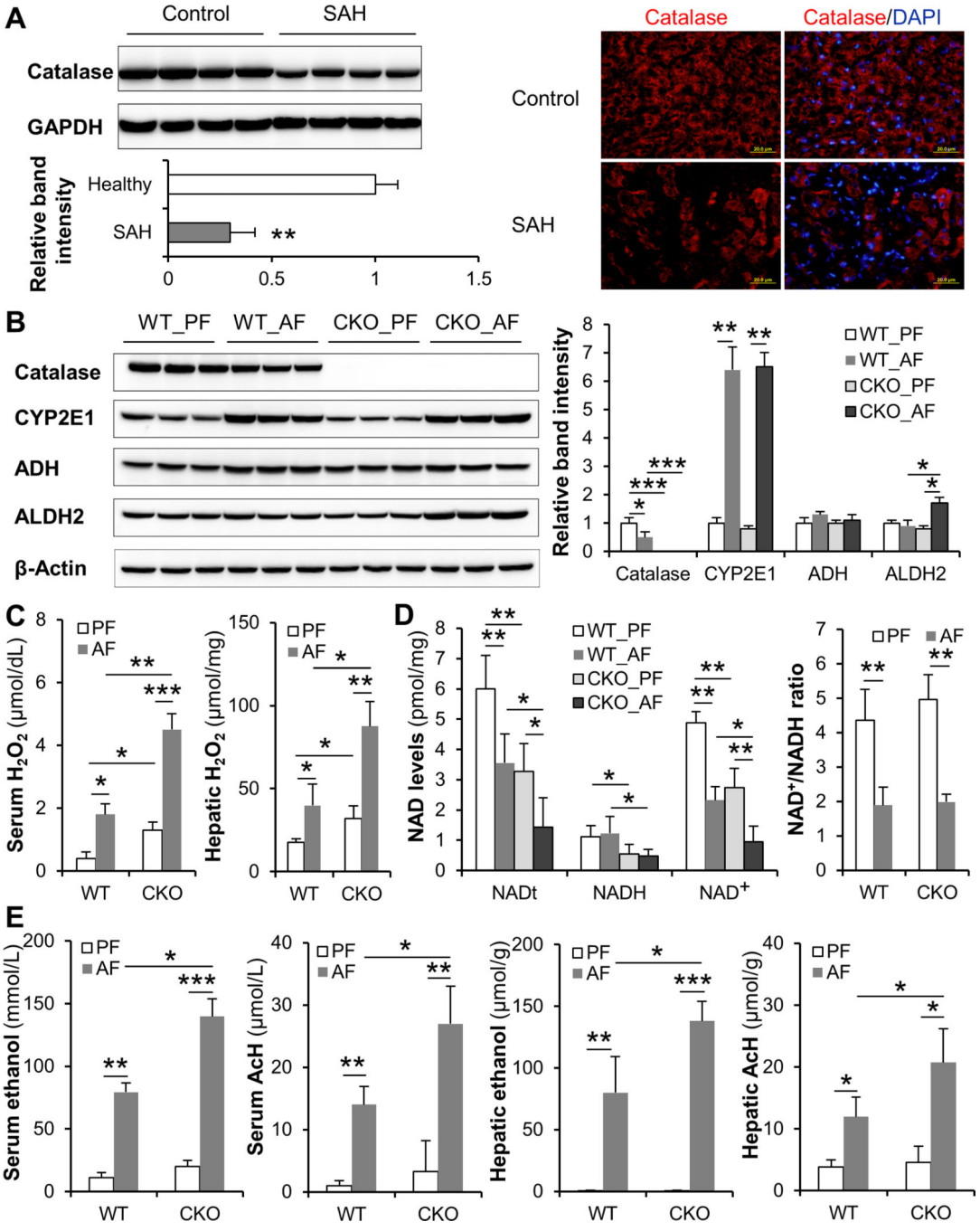

Figure 5. Catalase deficiency hampers alcohol and H_2O_2 removal in mice.

(A) Western blot and immunofluorescence staining of catalase in the livers of healthy subjects and patients with severe alcoholic hepatitis (n=4). WT and catalase knockout mice were pair-fed control or alcohol diet for 8 wks. (B) Representative Western blot bands and quantification of alcohol metabolizing enzymes CYP2E1, ADH, catalase and ALDH2. (C) Blood and hepatic H_2O_2 levels measured using Amplex Red H_2O_2 assay kit (n=6). (D) Hepatic NAD^+, NADH levels and NAD^+/NADH ratio (n=6). (E) Blood and hepatic ethanol

and acetaldehyde levels quantified by GC-MS (n=6). *P<0.05, **P<0.01, ***P<0.001. PF, pair-fed; AF, alcohol-fed; CKO, catalase knockout; AcH, acetaldehyde.

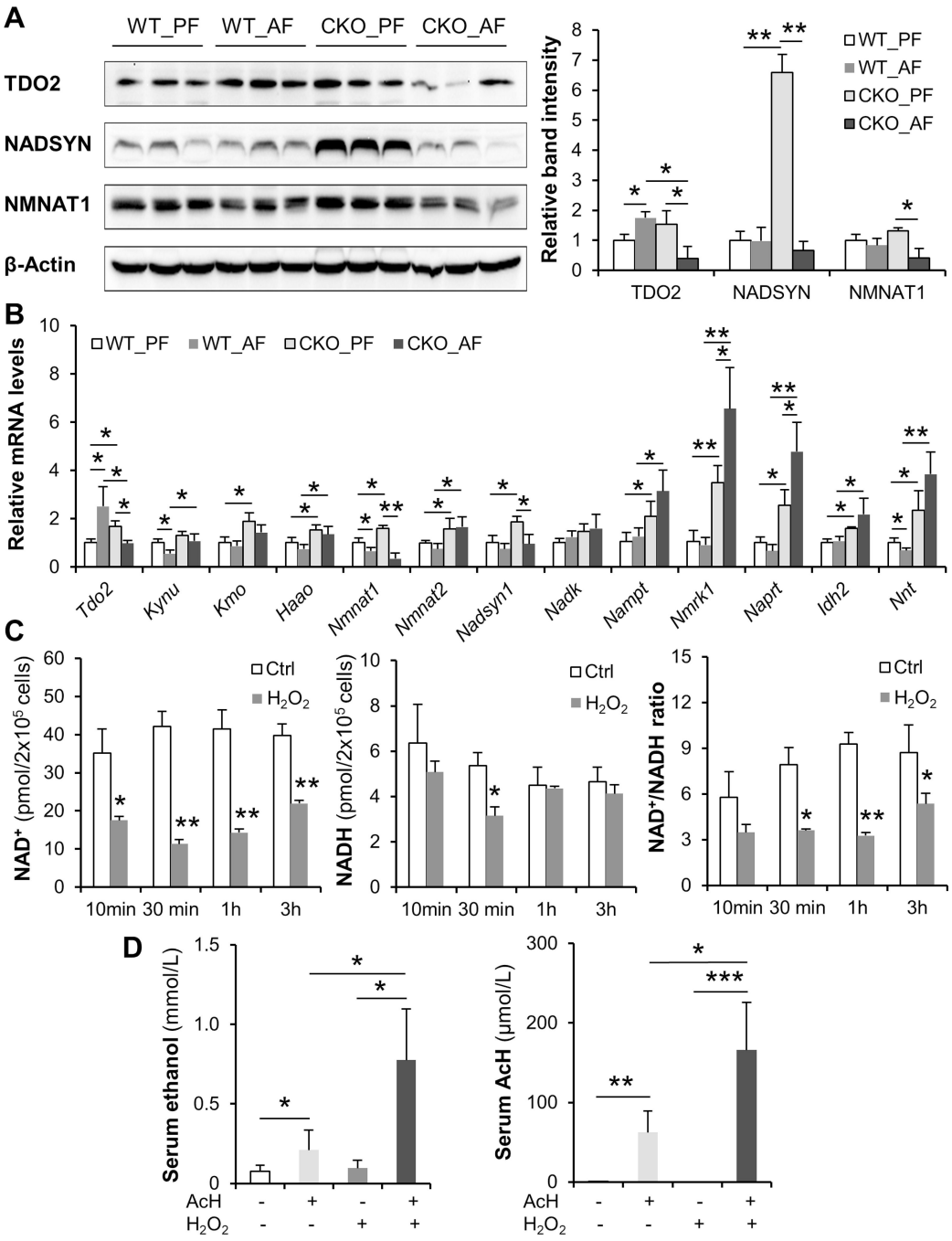

Figure 6. Hydrogen peroxide and alcohol synergistically perturb NAD biosynthesis enzymes and alcohol clearance.

WT and catalase knockout mice were pair-fed control or alcohol diet for 8 wks. (A) Representative Western blot bands and quantification of NAD biosynthesis enzymes TDO2, NADSYN, and NMNAT1. (B) mRNA levels of enzymes involved in NAD biosynthesis measured by qPCR (n=4). (C) Cellular NAD^+, NADH levels and NAD^+/NADH ratio in Hepa1c1c7 cells. Hepa1c1c7 cells were treated with 200 μmol/l H_2O_2 for up to 3 h. (D) Blood ethanol and acetaldehyde levels in mice quantified by GC-MS (n=6). WT mice were intraperitoneally injected with 100 mg/kg acetaldehyde, 100 mmol/l H_2O_2, or a combination

of acetaldehyde and H_2O_2 twice/d for 3 d. *P<0.05, **P<0.01, ***P<0.001. PF, pair-fed; AF, alcohol-fed; CKO, catalase knockout.

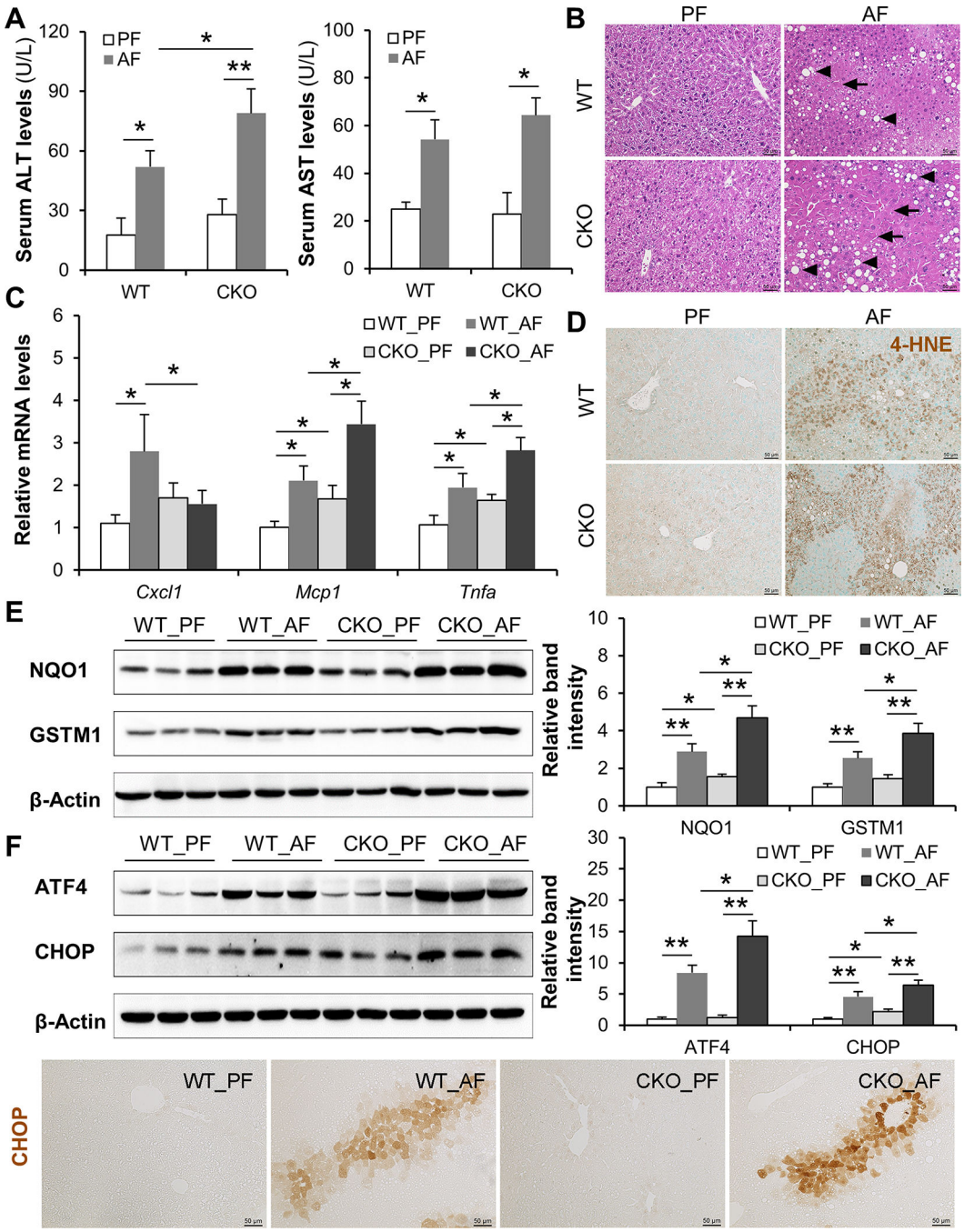

Figure 7. Catalase deficiency aggregates alcohol-induced liver damage in mice.

WT and catalase knockout mice were pair-fed control or alcohol diet for 8 wks. (A) Serum ALT and AST levels. (B) H&E staining of liver sections. Arrowheads indicate lipid accumulation and arrows indicate hepatocyte degeneration. Scale bar, 50 μm. (C) mRNA levels of hepatic cytokines and chemokines. (D) immunohistochemistry (IHC) staining of 4-HNE in liver sections. Nuclei were counterstained by methyl green. Scale bar, 50 μm. (E) Representative Western blot bands and quantification of hepatic NQO1 and GSTM1. (F) Representative Western blot bands and quantification of ER stress markers, ATF4 and

CHOP, in the liver. (G) IHC staining of CHOP in liver sections. Scale bar, 50 μm. *P<0.05, **P<0.01. PF, pair-fed; AF, alcohol-fed; CKO, catalase knockout.

Table 1.

Hepatic metabolites with significant difference between AF vs PF & AF+Wy vs AF in mice

Metabolite	HMDB ID	Class	Fold change (AF vs. PF)	*P* value	Fold change (AF+Wy vs. AF)	*P* value
Acetylcarnitine[a]	HMDB0000201	Fatty acid esters	0.66	4.1E-04***	4.29	9.7E-05***
2-Hydroxy-3-methylbutyric acid[a]	HMDB0000407	Fatty acids and conjugates	1.21	1.5E-03**	0.47	2.2E-08***
5,8,11,14,17-Eicosapentaenoic acid	HMDB0001999	Fatty acids and conjugates	0.53	1.1E-03**	0.47	1.6E-02*
Arachidonic acid	HMDB0001043	Fatty acids and conjugates	1.20	8.4E-03**	0.74	1.5E-03**
Decosahexaenoic acid	HMDB0002183	Fatty acids and conjugates	1.34	7.1E-03**	0.77	1.2E-02*
Myristic acid	HMDB0000806	Fatty acids and conjugates	2.03	8.7E-05***	0.25	7.8E-06***
Octadecanoic acid	HMDB0000827	Fatty acids and conjugates	1.36	4.9E-04***	0.72	6.6E-04***
Sebacic acid[a]	HMDB0000792	Fatty acids and conjugates	0.62	2.2E-03**	1.48	4.0E-04***
Gamma-Linolenic acid	HMDB0003073	Lineolic acids and derivatives	1.87	1.6E-04***	0.57	6.0E-04***
1-Monooleoylglycerol	HMDB0011567	Monoradylglycerols	1.87	1.4E-04***	0.25	1.3E-07***
1-Monopalmitin	HMDB0011564	Monoradylglycerols	1.38	1.7E-02*	0.63	6.8E-03**
1-stearoyl-rac-glycerol	HMDB0011131	Monoradylglycerols	1.25	3.5E-02*	0.80	1.4E-02*
2-Oleoylglycerol	HMDB0011537	Monoradylglycerols	1.35	1.9E-03**	0.34	2.8E-10***
Glycerol-3-phosphate	HMDB0000126	Glycerophosphates	0.62	5.4E-05***	1.46	7.7E-03**
Squalene	HMDB0000256	Triterpenoids	4.17	7.7E-07***	0.23	3.1E-06***
Adenosine-5-monophosphate	HMDB0000045	Purine ribonucleotides	0.58	6.0E-06***	1.46	2.7E-03**
4-Aminobutyric acid	HMDB0000112	Amino acids, peptides, and analogues	3.66	2.2E-06***	0.60	4.1E-03**
5-Oxoproline	HMDB0000267	Amino acids, peptides, and analogues	0.68	2.3E-06***	1.15	4.2E-02*
Aminomalonic acid	HMDB0001147	Amino acids, peptides, and analogues	0.64	8.1E-04***	1.47	1.9E-03**
Citrulline[a]	HMDB0000904	Amino acids, peptides, and analogues	0.59	1.1E-02*	1.66	6.8E-07***
Cysteine	HMDB0003417	Amino acids, peptides, and analogues	1.59	1.9E-02*	0.56	9.2E-03**
Delta-hydroxylysine[a]	HMDB0000450	Amino acids, peptides, and analogues	0.76	1.1E-03**	3.08	7.1E-15***
Glutamine	HMDB0003423	Amino acids, peptides, and analogues	0.69	2.9E-04***	1.22	1.9E-02*

Free Radic Biol Med. Author manuscript; available in PMC 2022 October 01.

Metabolite	HMDB ID	Class	Fold change (AF vs. PF)	*P* value	Fold change (AF+Wy vs. AF)	*P* value
Glutathione[a]	HMDB0000125	Amino acids, peptides, and analogues	0.27	5.0E-03**	3.41	2.2E-04***
Guanidinosuccinic acid[a]	HMDB0003157	Amino acids, peptides, and analogues	0.59	1.1E-02*	1.66	6.8E-07***
Histidine	HMDB0000177	Amino acids, peptides, and analogues	0.69	2.2E-04***	1.95	5.0E-06***
Homoserine[a]	HMDB0000719	Amino acids, peptides, and analogues	2.85	8.5E-08***	0.67	5.5E-03**
Leucine	HMDB0000687	Amino acids, peptides, and analogues	0.85	1.0E-02*	1.68	4.8E-08***
Methionine	HMDB0000696	Amino acids, peptides, and analogues	0.73	1.3E-02*	1.33	1.7E-02*
N6-Acetyl-L-lysine[a]	HMDB0000206	Amino acids, peptides, and analogues	1.51	2.2E-05***	0.61	9.4E-06***
N-acetyl-glutamine[a]	HMDB0006029	Amino acids, peptides, and analogues	2.11	8.2E-07***	0.54	1.8E-06***
Ornithine	HMDB0000214	Amino acids, peptides, and analogues	0.80	2.2E-03**	1.66	5.8E-06***
Phenylalanine	HMDB0000159	Amino acids, peptides, and analogues	0.79	1.2E-03**	1.37	7.5E-05***
Phosphoserine[a]	HMDB0000272	Amino acids, peptides, and analogues	0.90	4.1E-02*	1.29	5.7E-07***
Threonine	HMDB0000167	Amino acids, peptides, and analogues	0.80	5.1E-03**	1.40	7.3E-05***
cis-Aconitic acid[a]	HMDB0000072	Tricarboxylic acids and derivatives	0.58	3.5E-04***	1.66	8.8E-04***
Pyruvic acid [a]	HMDB0000243	Alpha-keto acids and derivatives	1.45	2.3E-02*	1.66	4.7E-03**
Succinylacetone[a]	HMDB0000635	Medium-chain keto acids and derivatives	0.88	2.3E-03**	1.30	3.7E-07***
Hypotaurine	HMDB0000965	Sulfinic acids	0.43	6.0E-04***	2.47	1.6E-06***
Acetylcholine[a]	HMDB0000895	Quaternary ammonium salts	0.82	7.7E-03**	1.13	1.9E-02*
Carnitine[a]	HMDB0000062	Quaternary ammonium salts	0.71	6.2E-04***	3.27	7.3E-15***
Phosphocholine[a]	HMDB0001565	Quaternary ammonium salts	0.72	5.0E-05***	1.37	1.2E-04***
Shikimic acid[a]	HMDB0003070	Alcohols and polyols	0.56	8.3E-07***	1.90	8.4E-05***
3-Phosphoglyceric acid	HMDB0000807	Carbohydrates and carbohydrate conjugates	2.14	2.7E-05***	2.27	8.5E-03**
6-Phosphogluconic acid	HMDB0001316	Carbohydrates and carbohydrate conjugates	0.42	5.7E-04***	0.66	4.3E-02*
Glucose	HMDB0000122	Carbohydrates and carbohydrate conjugates	0.64	4.8E-02*	1.62	3.9E-02*
Indoxyl glucuronide	HMDB0010319	Carbohydrates and carbohydrate conjugates	0.30	2.0E-02*	3.03	4.1E-04***
Ribonic acid	HMDB0000867	Carbohydrates and carbohydrate conjugates	1.87	5.0E-04***	0.74	2.6E-02*

Metabolite	HMDB ID	Class	Fold change (AF vs. PF)	*P* value	Fold change (AF+Wy vs. AF)	*P* value
Ribose 5-phosphate	HMDB0001548	Carbohydrates and carbohydrate conjugates	0.65	7.6E-03**	2.22	4.2E-02*
Urocanic acid	HMDB0000301	Imidazoles	0.44	7.7E-08***	0.43	1.0E-05***
2,5-bis-hydroxy pyrazine	HMDB0035284	Pyrazines	0.67	3.3E-04***	1.42	3.1E-03**
Thymine	HMDB0000262	Pyrimidines and pyrimidine derivatives	0.49	1.3E-05***	1.37	4.8E-03**
Uracil	HMDB0000300	Pyrimidines and pyrimidine derivatives	1.53	4.3E-04***	1.20	4.9E-02*
Ascorbic acid[a]	HMDB0000044	Furanones	0.34	1.1E-03**	1.94	4.5E-02*
Tryptophan[a]	HMDB0030396	Indolyl carboxylic acids and derivatives	0.88	8.2E-03**	1.29	7.3E-06***
Nicotinamide	HMDB0001406	Pyridinecarboxylic acids and derivatives	0.88	5.9E-03**	1.57	1.5E-06***

Note:

[a]indicates metabolites that were validated by standards.

*$P < 0.05$

**$P < 0.01$

***$P < 0.001$.